



J. Chem. Pharm. Res., 2011, 3(4): 589-595

ISSN No: 0975-7384
CODEN(USA): JCPRC5

Altering the electronic properties of adamantane through encapsulating small particles

Z. Bayat* and M. Jalroshan

Department of Chemistry, Islamic Azad University Quchan Branch, Iran

ABSTRACT

The stability, optimized structure, binding energy, dipole moment and electronic gap of adamantane, $C_{10}H_{16}$, incorporating cage-centered small atoms and ions ($X@$ cage, where $X = Li^{0,+}$, Be^{2+} , $Na^{0,+}$, Mg^{2+} , He, and Ne) have been studied at the B3LYP hybrid level of theory. A wide variety of atoms and ions can be encapsulated by adamantane. The complexes are more stable for smaller and more highly charged metallic guest species. The electronic HOMO–LUMO gaps of adamantane complexes are significantly affected by the inclusion of charged particles. The stability of the structures, the amount of the charges which are transferred between small particles and adamantane cage, and the change in the HOMO–LUMO gaps of adamantane complexes are nearly the same for the corresponding possible complexes. All these features mostly depend on the charge, the size and the type of the encapsulated particle. It is well recognized that the energy difference between highest occupied molecular orbital (HOMO) and the lowest unoccupied molecular orbital (LUMO) known as HOMO–LUMO gap (HLG) is a key parameter determining the conductance property. This parameter calculated for molecules and complexes.

Keywords: Adamantane, Cage, Homo, Lumo, Binding Energy, Dipole Moment.

INTRODUCTION

The smallest possible diamondoid is adamantane tricyclo [3,3,1,1] decane, consisting of 10 carbon atoms arranged as a single diamond cage, surrounded by 16 hydrogen atoms, as shown in figure 1.

Designing nano scale building blocks and engineering their optoelectronic properties is one of the most rapidly evolving fields of nanomaterials. The recognition of diamondoids and their derivatives as suitable building blocks for nanotechnological devices has sparked an interest in both calculating and measuring their optoelectronic properties [1]. Given that diamondoids are nano-sized hydrogen terminated diamond fragments, it was anticipated that reducing the size of

diamond to the nano-scale would have a strong effect on its optical gap. According to the quantum confinement (QC) model, with decreasing particle size the energy gap between the lowest unoccupied molecular orbital (LUMO) and the highest occupied molecular orbital (HOMO) increases.

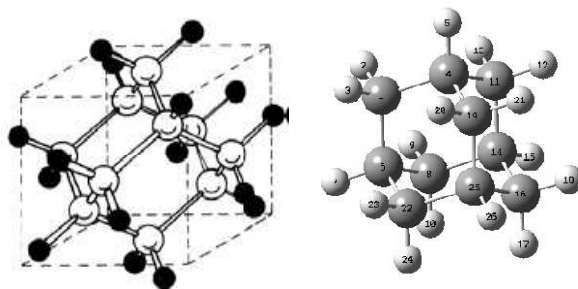


Fig. 1. The structure of a adamantane molecule

Diamondoids are classed with organic nanostructures [2] and Bulk diamond has a large band gap, so it is expected that the HOMO–LUMO energy gap of diamondoids will be pushed further into the UV range. This could be applied in a new generation of UV sensors. Consequently, many recent theoretical and experimental studies have been performed to investigate the optoelectronic properties of these molecules [3–6]. However, diffusion quantum Monte Carlo (DMC) [6], along with density functional theory (DFT) calculations with both plane-wave and diffuse Gaussian basis sets [3, 6], show that, in contrast to Si and Ge nanoclusters, QC effects disappear in diamondoids larger than 1 nm. According to [3] and [6], for a diamond nanoparticle larger than 1 nm, the HOMO–LUMO energy gap is even smaller than the gap of bulk diamond. This result has been confirmed by further experimental investigation of the soft x-ray absorption and emission spectra [7, 8]. The spectra from x-ray absorption spectroscopy (XAS) show that diamondoids exhibit negligible shifting in the LUMO levels and the changes in HOMO–LUMO energy gap stem only from QC effects in the HOMO levels. Therefore diamondoids do not seem likely to be as useful as was earlier predicted for UV sensor applications. One possible way of overcoming this problem is to use diamondoid derivatives.

First-principles studies have shown that when residues like Na are added, their electronic properties, such as the HOMO–LUMO gap or the electrical conductance, can be changed. It has also been demonstrated that the quantum conductance of diamondoid molecules and their derivatives changes significantly when their orientations are changed [9]. This has given rise to a new branch of materials for application in nanoelectro-mechanical systems and micro-electro-mechanical systems.

On the other hand, it has also been shown that incorporating charged species into silicon fullerene clusters enables their optoelectronic properties to be tuned [10–12]. This motivated us to explore another idea: whether the encapsulation of small ions in the adamantane cage could yield stable adamantane complexes ($X@cage$, where $X = Li^{0,+}$, Be^{2+} , $Na^{0,+}$, Mg^{2+} , He, and Ne), and whether this would affect the electronic properties of these nanostructures. To answer this question we have performed theoretical calculations using the DFT method for adamantane ($C_{10}H_{16}$). Adamantane, belong to the T_d point group. We have investigated the effect of encapsulating different small cage-centered endohedral particles on the stability and electronic gap of these molecules. We have sought to find how the HOMO–LUMO energy gap of adamantane complexes changes as a function of the size and, charge, and type of the guest particles. The stabilities of the endohedral minima of adamantane complexes have been evaluated by comparing their energies to the sum of the energies of their isolated components.

Our results demonstrate that in molecules, the stability of the encapsulated complex is greatest for small, highly charged metallic particles such as Be^{2+} . The calculated natural charges indicate that a significant amount of electronic charge density is transferred between the cage's atoms and the central particle. This results in a Coulomb interaction between the cage and the encapsulated particle, and also polarizes the complex, thereby altering the electronic properties of adamantane complexes considerably.

The electronic conduction has been analyzed from the change in the shape of molecular orbitals and the evolution of the HOMO–LUMO gap of the adamantane and $\text{X}@C_{10}H_{16}$ complexes under the influence of the electric field.

2. Computational methods

Adamantane complexes were optimized at the B3LYP/6-31G(d, p) level of theory. B3LYP is Becke's three parameter hybrid functional [14], which uses the non-local correlation provided by the LYP expression [15]. The B3LYP functional was chosen because mixing in a fraction of exact exchange leads to the cancellation of self-energy errors. Since the highest angular momentum orbital for hydrogen and carbon are s and p states, respectively, the polarizations of the atoms were described by adding sets of p and d functions. According to [6], the LUMO in Adamantane is a delocalized state with a considerable charge outside of the H atoms terminating the surface. So it is advantageous to augment the basis set with diffuse functions, i.e. functions that have smaller orbital exponents than those normally used. Concern for this characteristic behavior of Adamantane is particularly important for the investigation of properties which are related to the optical gaps of these molecules. Consequently, the 6-31G(d, p) basis set was used throughout this work to optimize the geometry of the complex.

In table 1 the optimized endohedral complexes were used to calculate Binding energy, Dipole moment and HOMO–LUMO gaps at the B3LYP/6-31G(d, p) level. The outcomes of the calculations were utilized to construct orbital interaction diagrams. All calculations were carried out using GAUSSIAN 03 program. [16, 17]

RESULTS AND DISCUSSION

3.1. Stability of the Adamantane-complex structures

The adamantane is good host cage, because the majority of the related endohedral complexes are minima (see figure 2). In our study (Li^{0+} , Be^{2+} , Na^{0+} , Mg^{2+} , He, and Ne) can be encapsulated by Td symmetric adamantane. The HOMO and LUMO of some adamantane complexes and a simple cage for comparison are shown in figure 3. The most stable complex, $\text{Be}^{2+}@C_{10}H_{16}$, has the most similar HOMO and LUMO iso surface to the corresponding iso surface of the single cage.

The HOMO iso surface plots of the complexes encapsulating metallic species do not change significantly relative to the HOMO iso surface of the single cage. The LUMO iso surface plot of $\text{Mg}^{2+}@C_{10}H_{16}$ is stretched from the hydrogen terminated surface to the cage center, where the relatively large and also highly charged ion is placed. We have also constructed the orbital interaction diagrams to explain how the stability of the structure relates to the type of the enclosed particle. However, $\text{Be}@C_{10}H_{16}$ is a stable structure; figure 4 shows the repulsive four-electron, two-orbital interaction reduces the stability of the complex. This is accompanied by a reduction in the HOMO–LUMO gap compared to the simple cage. The interaction of the A1 symmetric level of $C_{10}H_{16}$ keeps the A1 orbital of $\text{Be}@C_{10}H_{16}$ below the T2, and ensures that the ground state is a closed shell singlet. In contrast, the positive charge of Be^{2+} lowers all of the

adamantane orbitals and increases the stability and the HOMO–LUMO gap. With this method we have found that a wide variety of atoms and ions, including $\text{Li}^{0,+}$, Be^{2+} , $\text{Na}^{0,+}$, He and Ne, can be enclosed by this molecule.

Table 1. The Binding Energy at B3LYP/6-31G(d, p) level for adamantane complexes, Dipole Moment, E HOMO, E LUMO, HLG(gap), Spin, and Point group.

NO	Molecule	E(ev)	D.M(debye)	E HOMO(ev)	E LUMO(ev)	HLG (ev)	Spin	P.G
1	$\text{C}_{10}\text{H}_{16}$	-10658.423	0.0001	-7.4507	1.8922	9.3429	Singlet	C1
2	$\text{Li}@\text{C}_{10}\text{H}_{16}$	-10856.487	0.0072	-0.5584	0.4981	1.0565	Doublet	C1
3	$\text{Li}^+@\text{C}_{10}\text{H}_{16}$	-10854.617	0.0054	-12.7932	-3.2001	9.5931	Singlet	C1
4	$\text{Be}^{2+}@\text{C}_{10}\text{H}_{16}$	-11037.346	1.9341	-17.7467	-7.6891	10.0576	Singlet	C1
5	$\text{Na}@\text{C}_{10}\text{H}_{16}$	-15069.044	0.0042	-0.9814	-0.1034	0.8780	Doublet	C1
6	$\text{Na}^+@\text{C}_{10}\text{H}_{16}$	-15066.892	0.0018	-12.6361	-3.3209	9.3152	Singlet	C1
7	$\text{Mg}^{2+}@\text{C}_{10}\text{H}_{16}$	-16089.813	0.0028	-17.7573	-7.6716	10.0857	Singlet	C1
8	$\text{He}@\text{C}_{10}\text{H}_{16}$	-10731.117	0.0025	-7.6152	2.2956	9.9108	Singlet	C1
9	$\text{Ne}@\text{C}_{10}\text{H}_{16}$	-14158.106	0.0194	-7.5304	2.3221	9.8525	Singlet	C1

It is predicted that the encapsulation of smaller and more highly charged metallic species at the center of the molecules is the most favorable. The most stable complex occurs for $\text{X} = \text{Be}^{2+}$. Be^{2+} is the smallest metallic charged species in our study.

If a Adamantane complex is a possible structure, its stability will largely depend on the type and charge of the encapsulated particle.

3.2. Optimized structures

Table 1 gives a comparison of the energy levels of HOMO and LUMO as well as their gap (HLG) and dipole moment for 9 molecules.

The calculated HOMO and LUMO energies show the charge transfer occurs in the molecules [18]

The optimized C–C and C–H bond lengths for $\text{X}@\text{cages}$ are summarized in table 2. Reviewing this table, it is obvious that, compared to the corresponding single cage, the C–C bond lengths of $\text{X}@\text{C}_{10}\text{H}_{16}$ have been stretched from their initial values of 1.543 Å.

The donation of electron density from the encapsulated particle into the cages' atoms stretches the bond lengths.



Figure 2. Structure of $\text{X}@\text{C}_{10}\text{H}_{16}$

MOLECULE	HOMO	LUMO
$C_{10}H_{16}$		
$Li^+@C_{10}H_{16}$		
$Be^{2+}@C_{10}H_{16}$		
$Na^+@C_{10}H_{16}$		
$Mg^{2+}@C_{10}H_{16}$		

Figure 3. The HOMO (left) and LUMO (right) isosurface plots of adamantane and $X@C_{10}H_{16}$ complexes.

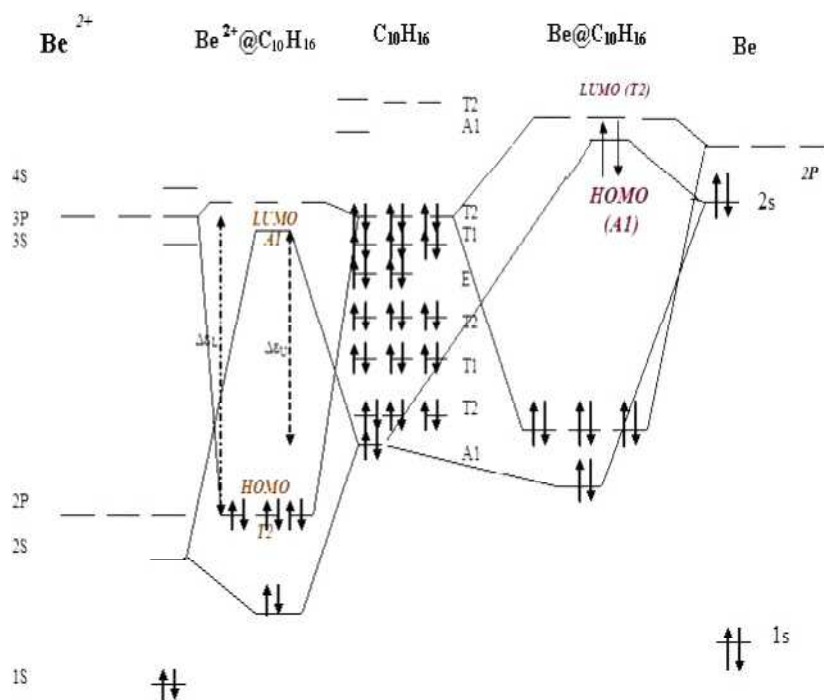


Figure 4. Orbital interaction diagrams for $Be^{0,2+}@C_{10}H_{16}$. The energy interval and symmetries of the levels were obtained from Gaussian 98 NBO output files.

Table 2. B3LYP/6-31G optimized C–C, C–H, and C–X bond lengths of X@C₁₀H₁₆ in Å°, and at the B3LYP/6-31G(d, p) level of theory. C(H), and C(H2) represent those carbons which are involved in the C–H and H–C–H antibonding, respectively.**

Bond	Single cage	Li@	Li ⁺ @	Be ²⁺ @	Na@	Na ⁺ @	Mg ²⁺ @	He@	Ne@
C(H ₂)–C(H)	1.543	1.616	1.623	1.628	1.745	1.751	1.755	1.607	1.735
C(H)–H	1.097	1.091	1.086	1.086	1.089	1.086	1.085	1.098	1.099
C(H ₂)–H	1.098	1.096	1.092	1.091	1.094	1.091	1.090	1.097	1.096
C(H)–X		1.644	1.651	1.646	1.795	1.801	1.803	1.623	1.778
C(H ₂)–X		1.849	1.858	1.868	1.984	1.990	1.997	1.845	

3.3. HOMO–LUMO gaps

The corresponding molecular orbital pictures for adamantane and X@C₁₀H₁₆ complexes obtained from their optimized geometries are visualized in figure 3. The application of EF may increase the molecular conjugation and the induced dipole moment, while decrease the HOMO–LUMO gap. In comparison with Si nanoparticles [13], including charged particles at the centers of diamondoids has a significant effect on their HOMO–LUMO gaps. The interaction of the cage and the charged particle completely changes the calculated gap of the cages. As expected, the greatest variation in complexes encapsulating metallic species occurs for more highly charged particles. The relative changes in the HOMO–LUMO gap due to including charged particles at the Td center of the Si₁₀H₁₆ cage from [13] are also added to this figure, and show how much more diamondoid cages are affected by the Coulomb interactions.

CONCLUSION

According to our studies, We could that conclude when one atom or ion are added to adamantane molecule, the electronic properties of adamantane can change such as the HOMO-LUMO gap of molecules, the conductance, etc. We have investigated the possibility of including small particles, including ions and atoms, at the center of adamantane, C₁₀H₁₆ (Td). These complexes are more stable for smaller and more highly charged metallic particles. The Coulomb interaction between charged guest species and cage affects their electronic properties, and represents a possible approach for engineering their HOMO–LUMO gap. These results could be applied in the optical engineering of nanodiamond devices, e.g. for use in UV sensors.

REFERENCES

- [1] Mansoori G A **2007** *Adv. Chem. Phys.* **136** 207–58
- [2] Z. Bayat and M. Fakoor Yazdan Abad, *J. Chem. Pharm. Res.*, 3(1), 48 (**2011**)
- [3] Raty J Y, Galli G, Bostedt C, van Buuren T W and Terminello L J **2003** *Phys. Rev. Lett.* **90** 037401
- [4] McIntosh G C, Yoon M, Berber S and Tom´anek D **2004** *Phys. Rev. B* **70** 045401
- [5] Lu A J, Pan B C and Han J G **2005** *Phys. Rev. B* **72** 035447
- [6] Drummond N D, Williamson A J, Needs R J and Galli G **2005** *Phys. Rev. Lett.* **95** 096801
- [7] Willey T M *et al* **2005** *Phys. Rev. Lett.* **95** 113401
- [8] Willey T M *et al* **2006** *Phys. Rev. B* **74** 205432
- [9] Xue Y and Mansoori G A **2008** *Int. J. Nanosci.* **7** 63
- [10] Kumar V **2004** *Comput. Mater. Sci.* **30** 260
- [11] Pichierri F, Kumar V and Kawazoe Y **2005** *Chem. Phys. Lett.* **406** 341
- [12] Zhang C-Y, Wu H-S and Jiao H **2005** *Chem. Phys. Lett.* **410** 457
- [13] Pichierri F **2006** *Chem. Phys. Lett.* **421** 319
- [14] Becke A D **1993** *J. Chem. Phys.* **98** 5648

- [15] Lee C, Yang W and Parr R G **1988** *Phys. Rev. B* **37** 785
- [16] S. Qanei Nassab, Z. Bayat and J. Movaffagh, *J. Chem. Pharm. Res.*, 3(1), 64 (**2011**)
- [17] Z. Bayat and S. Vahdani, *J. Chem. Pharm. Res.*, 3(1), 93 (**2011**)
- [18] P. Udhayakala, T. V. Rajendiran, S. Seshadri and S. Gunasekaran, *J. Chem. Pharm. Res.*, 3(3), 610 (**2011**)